Journal of Engineering and Science Research 7 (2): 12-19, 2023
e-ISSN: 2289-7127

DOI: 10.26666/rmp.jesr.2023.2.3

# Polyvinyl Alcohol (PVA) Hydrophilic Behaviour of Porosity Condition for 3DPrinted Medical Splinting Devices

*Abdraman Hassan Malloum[1,a], Muhammad Aiman Ahmad Fozi[2,a], Mohd Zamzuri Mohammad Zain[3,a], Muhammad Hasnulhadi Mohammad Jaafar[4,a], Mohd Azaman Md Deros[5,a]*
[a]Faculty of Mechanical Engineering & Technology, Universiti Malaysia Perlis, Pauh Putra Main Campus, 02600 Perlis, Malaysia.



*Received: 20 February 2023; Revised: 26 February 2023; Accepted: 20 March 2023; Published: 30 April 2023*

**Abstract:** The splint is one of the methods used to treat misalignment, deformations, broken limbs, and others. The breathable condition for splinting is essential for reducing the implications of the contact between human skin and the splint itself. Previous splinting fabrication apparatus in a local hospital used low thermoplastic material with no porosity. This material cannot provide breathable conditions for human skin due to low porosity. Low thermoplastic material without porosity will cause implications such as itchiness, sweats, and uncomfortable circumstances. To overcome the problem of low porosity, a new material with sufficient porosity needs to be developed. Nowadays, the use of 3D printing is increasing in medical sectors where customized items are the best solution to fit the differences of human anthropometry. Therefore, new materials such as Polylactic Acid (PLA) and Polyvinyl Alcohol (PVA) are being developed to suit the needs of particular applications. In this study, PLA/PVA melt bending method is applied to fabricate 3D printed medical splinting devices. The physical, mechanical and morphology properties are also investigated. The results revealed that a porous structure was successfully formed by mixing PLA with various volume fractions of PVA. The porosity of PLA sample before mix blending was found to be 3.57%, and increased to 18.52%, 33.3% and 37.0% as the volume fraction of PVA is increased to 30,40 and 50 respectively. The tensile results show that the force increased with increase in PVA percentage and the highest force recorded for the sample of 30% was 52.1 N. The 3D printer successfully printed the composite finger splint device. This paper demonstrates the feasibility of transforming biodegradable PLA into porous products, contributing to better medical splint appliances and additive manufacturing players in Malaysia.

**Keywords:** *polylactic acid (PLA), polyvinyl alcohol (PVA), biomedical applications, scaffolds, tissue engineering, 3D printing, polymer lend, 3D printing, porosity, splinting device.*

## INTRODUCTION

Nowadays, 3D Printing is growing rapidly with the advancement of variables of materials and technology. Beside big data cloud-based systems and other wireless implementations in IR 4.0, additive manufacturing is one of the apparatuses that will be a game-changer in manufacturing processes. Most medical care is custom-made to fit patients' anthropometry [1]. Reverse engineering is used to obtain the dimension of particular parts to develop the product using additive manufacturing technologies. Referring to the Occupational Therapist (OT) unit in a hospital, most of the items used in the treatment mainly were tailored to each patient differently. It is to suit the patient and provide better-healed results. The splint is used to treat broken, misaligned, and deformation of limbs [2]. The improvement of splints has evolved from using weighty materials to lightweight materials [3].

Custom-fitting splints have several practical and aesthetic drawbacks because they are typically handmade from sheets of low-temperature thermoplastic (LTT). The standard LTT splint is made of solid hard plastic when it is created. Velcro and other bulky fasteners, including big buckles, can

**Corresponding Author:** Muhammad Aiman Ahmad Fozi, Mechanical Engineering Program, Faculty of Mechanical Engineering Technology, Universiti Malaysia Perlis, Pauh Putra Main Campus, 02600 Arau, Perlis, Malaysia, aiman@unimap.edu.my

be incorporated. Regarding appearance, patients could feel stigmatized by using assistive technology [4]. Patients have problems keeping their splints clean and dry and with inadequate skin ventilation in terms of function and practicality, particularly in the palmar region, which has about 500 eccrine sweat glands per square centimeter [5].

Polyvinyl Alcohol (PVA) is mainly used as support material in FDM 3D printing processes. Its hydrophilic behavior is suitable as a support material for complex shapes in building components from ABS, PLA, and other materials. The PVA support material will disappear over time and leave the final product [6]. Polylactic Acid (PLA) polymer is known as biodegradable material used widely in 3D printing. Therefore, this study is dedicated to investigating the role of PVA in developing porous material through a combination of both PLA and PVA matrices.

A low-temperature thermoplastic sheet is used to construct the splint. However, low-temperature thermoplastic splinting materials cannot provide breathable conditions for human skin due to low porosity [7]. Low porosity will cause implications between the contact of human skin and the splint's surface. A previous study has reported that a customized 3D printing padding used to increase pressure for hypertrophic scars treatment caused several implications due to low porosity. The authors suggest that a breathable pad should be developed to alleviate any impact of padding applications [8].

The concerns with open cell padding absorbing moisture and collecting sweat. Splints created using traditional techniques are currently exceedingly challenging to keep clean and dry because they accumulate sweat and humidity, which can lead to an unsanitary splint. To avoid potential distortion or trouble drying the splint, patients may be instructed to wash their splints by hand using mild detergents like washing liquid or, depending on the materials used, may be required to forgo cleaning the splint altogether. Initial research by Paterson, however, indicated that practitioners were receptive to novel ideas for splint design and fabrication using three-dimensional (3D) computer-aided design (CAD) to assist additive manufacturing (AM) [9].

For instance, due to their distinct advantages, including biodegradability and thermal and mechanical capabilities, PLA/PVA blends can be considered for various applications, including medical, packaging, agriculture products, adhesive, and coatings. Saini et al. discussed several biomedical uses for PLA/PVA mixes, including drug delivery, tissue engineering, and implants. [10]. The porous structure to be formed melt blending method is highly recommended [11]. The fabrication of orthoses and splints is a potentially easy application in 3D printing. Several studies and case reports have proposed different design algorithms for 3D printing splints and assistive devices for hand surgery [12]–[17].

Essentially, this study would assist in understanding the correlation between process parameters, filament properties and performance of final 3D printed products. The knowledge integration between material and performance aspects will increase the implementation of additive manufacturing in various sectors. Finally, the research vision is to produce a splinting device with a higher porous structure using AM technique (3D printing) with composite polymer instead of the traditional method, which is a handmade low thermoplastic material.

Breathable condition is essential in increasing comfort and reducing patient implications [18], [19]. However, the material capable of producing porous splinting remains unresolved. Thus, this study aims to produce a porous splinting device that can be used directly using additive manufacturing technology at a low cost (FDM 3D printer). Furthermore, the porosity can be achieved via water dispersion at the post-processing stage.

## MATERIALS AND METHOD

The methodology used in this investigation consists of three processes starting with 3D printing the composite, phase separation process, mechanical test, and microstructure characterization.

### Materials

Polylactic acid (PLA) filament was purchased from Fabbxible Technology (PG0382404-A) and polyvinyl alcohol (PVA) filament was supplied by Torwell Technologies Co. The specification is illustrated in Table 1.

Table 1: The specification of PLA and PVA.

| Property | PLA | PVA |
|---|---|---|
| Physical state | Solid | Solid |
| Appearance | Clear | Clear |
| Color | White | Nature |
| Density | 1.25 | 1.19-1.31 |
| Melting point/ melting range | 190-220 | 190-220 |
| Water solubility | Insoluble | Soluble |

### 3D Printing Sample Preparation

The printing process consisting of PLA/PVA filament mixture was conducted using A10M 3D printer from Geeetech with mixing capability to achieve the research objective. Samples of dumbbell shapes were printed to conduct the mechanical testing and square shape for microstructure characterization. The printing parameters for the printing process are as shown in Table 2. The samples are named S1, S2 and S3 for PLA/PVA volume fraction of 70/30, 60/40 and 50/50 respectively. The sample dimension was according to ASTM D638 standard for tensile test [20].

Table 2: The parameter settings for samples

| Code | PLA/PVA, % | Temp, ℃ | Speed, mm/s | Infill, % |
|---|---|---|---|---|
| PLA | 100/0 | 210 | 60 | 100 |
| S1 | 70/30 | 210 | 60 | 100 |
| S2 | 60/40 | 210 | 0 | 100 |
| S3 | 50/50 | 210 | 60 | 100 |

**Phase Separation Process**

In this stage, the samples were submerged in distilled water to allow the PVA to dissolve and leave the voids structure inside the samples. All samples were immersed in distilled water at room temperature and stirred at 700 rpm for 24 hours. Then the samples were dried from moisture in the oven for 24 hours at a constant temperature of 40℃. Then, the samples are ready for SEM imaging for morphology characterization, tensile test for mechanical testing and porosity investigation. Thereafter, the sample was weighted (m) to calculate the dissolved PVA content (ω) by equation (1) [21].

$$\omega = \left(\frac{m0-m}{m0}\right) \times 100 \qquad (1)$$

**Morphology**

The samples were observed by using Scanning electron microscopy (SEM) at 10 kV and samples were coated with magnesium to collect a higher magnification due to low conductivity of PLA/PVA.

**Tensile Strength**

The samples were printed, and its tensile strength were characterized and evaluated by using a universal testing machine according to ASTM D638 standard.

**Density**

The density (D) was measured by a densimeter machine, which is based on the Archimedes principle and expressed in equation (2), which is a relationship between mass (M) divided by the volume (V).

$$D = \frac{m}{v} \qquad (2)$$

**Porosity**

Porosity is defined as the ratio of void volume and total volume and is expressed in equation (3), which is a relationship between before (ρ0) and after (ρ) etching density of the sample [22].

$$\emptyset = \left(1 - \frac{\rho}{\rho 0}\right) \times 100 \qquad (3)$$

**RESULT AND DISCUSSION**

**Surface Morphology by SEM**

Due to the effectiveness of the phase separation procedure, the initial observation (naked eye) of all samples before and after the water submersion process were entirely different. Furthermore, the observation through SEM has validated the initial observation by naked eye. Figure 1 shows the SEM images of PLA/PVA samples with different volume fractions before and after the phase separation procedure. Samples before the phase separation procedure (B30~B50) exhibit long and thin voids during the phase separation process co-continuous structure was formed [23]. The shape of the micro was altered due to the successful etching of PVA with distilled water voids depending on the production method, the extruded samples a sea-island morphology [22]. In the image of the 40 percent sample (A40), the PVA continues to dissolve in the distilled water, and the voids are becoming more profound and more significant compared to the image of the 30 percent sample (B30).

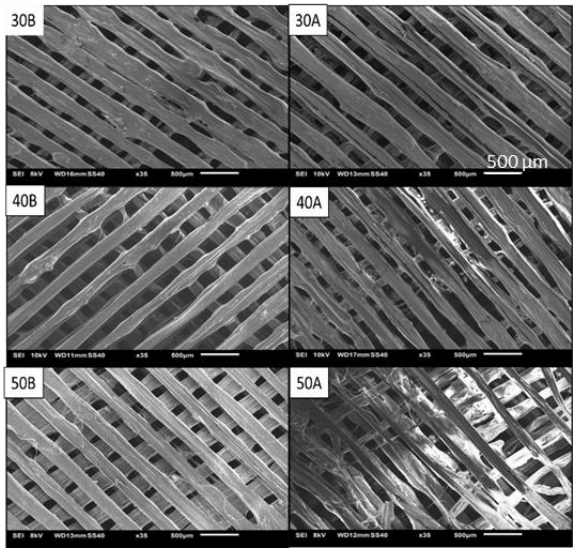


Figure 1:Morphology surface of 50%, 40%, and 30% samples before (B) and after (A).

It was also observed that water also penetrated the third sample (A50), and the voids are thinner and smaller than the last samples. whereas (A30), (A40), and (A50) exhibit the samples after the phase separation process The image demonstrates that the layer of this sample is becoming thinner and weaker compared to the (B50) sample, which has a PVA concentration of 50 percent. This sample's tensile test indicated the most fragile maximum force value compared to the other samples. The subsequent findings are weight changes, density, and porosity will justify and support this study's morphological photos and tensile testing.

**Tensile Test**

A tensile test was conducted to determine the maximum force, displacement, strain, and stress. The samples used according to the ASTM standard D638[24][25]. Figure 2 and 3 show the force and displacement before and after phase separation, strain, and stress. The graph illustrates the difference between the tensile test values and the PVA's effectiveness in the structure of the 3D printed samples.

Figure 2 shows the graph of all samples' maximum force and displacement before the phase separation process. The sample of the 100% PLA offers the highest point recorded in the entire area is 75.4 N due to the absence of the PVA element in this sample. Second, the sample of the 30% shows a higher value of the maximum force is 57.5 N compared to the other sample containing a higher PVA ratio. From the graph, the sample of the 40% recorded 48.3 N, an almost similar value of the maximum force compared to the following sample. The sample of the 50% recorded the lowest value of the maximum force, only at 46.2 N, due to the highest amount of the PVA ratio. The tensile test results showed that the more PVA content, the lower the maximum force recorded. The PVA content significantly affects the structure of the 3D printed sample before the phase separation process.

Figure 3 shows the graph of all samples' maximum force and displacement after the phase separation process. The result shows that the force increased with increase in PVA percentage. However, the force decreases when the ratio of PLA/PVA is 50%. The highest force recorded for the sample of 30% was 52.1 N. According to these results, it can be concluded that the decreasing in force was related to increasing porosity in the microstructure.

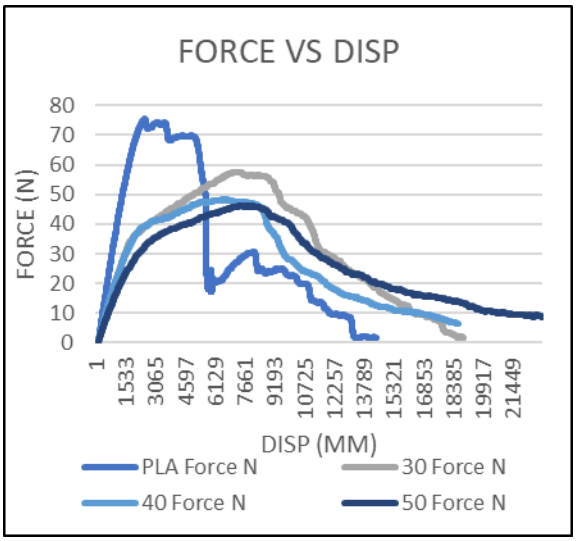


Figure 2: Force and displacement before the phase separation process.

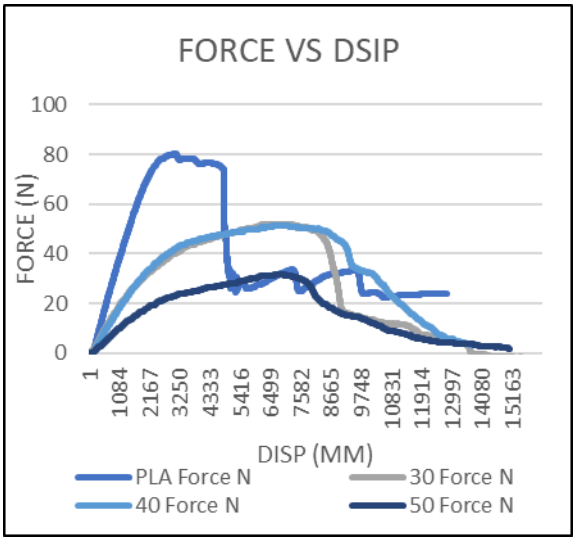


Figure 3: Force and displacement after the phase separation process.

Figure 4 and 5 show the graph of the maximum stress and strain of all samples before and after the phase separation process. The results show that the stress value gradually decreased with the increase of PVA percentage. The stress values before phase separation were 7.4, 5.6, 4.7, 4.5 N/mm$^2$ when PLA/PVA ratio were 100, 30, 40, 50% respectively. While, after the phase separation process, the stress value shows 7.9, 5.1, 5.0, 3.1 N/mm$^2$ for the respected PLA/PVA ratio. The stress and stress are almost unchanged irrespective of presence of PVA in the sample especially with 30% and 40% ratio.

.

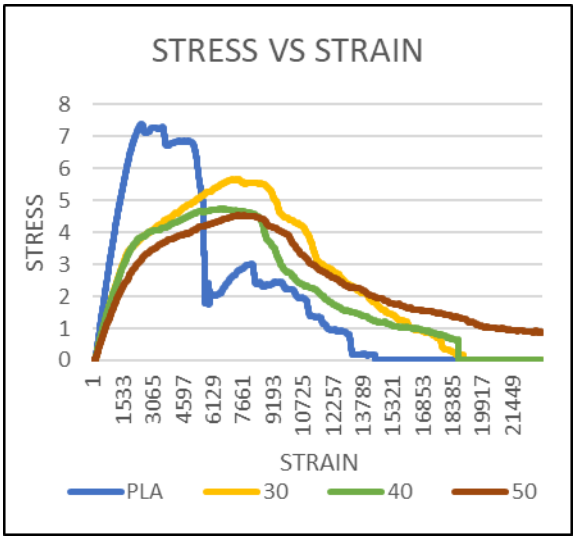


Figure 4:stress and strain before the phase separation process.

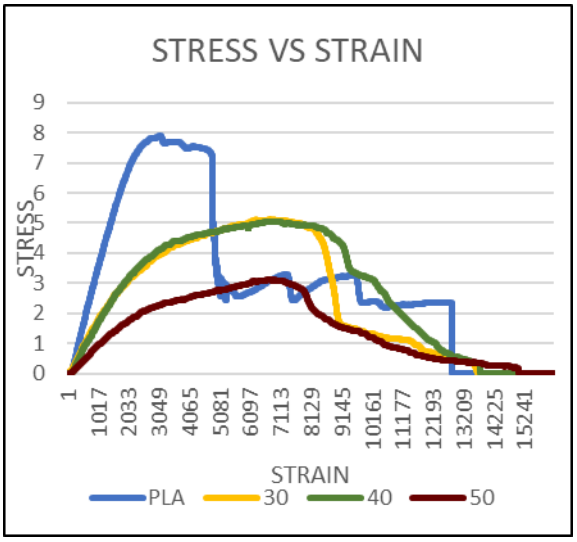


Figure 5:stress and strain after the phase separation process.

**Porosity Investigation**

Figure 6 shows the graph of the weight changes of all the samples. The diagram indicates that more PVA added to the composition, more weight loss could be observed due to the etching process. The weight loss of the 100% PLA sample was almost unchanged with 0.1 g after the phase separation process. The weight loss values increase as the PVA content increases in the sample. PVA is likely to dissolve in water during the phase separation process and it produces porosity in the microstructure. This result corresponds with the morphology images and the tensile test due to the effectiveness of the PVA ratio.

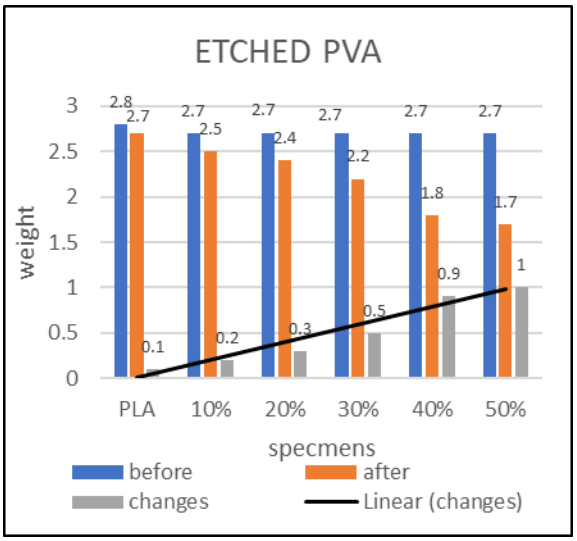


Figure 6: weight changes before and after the water submerged process.

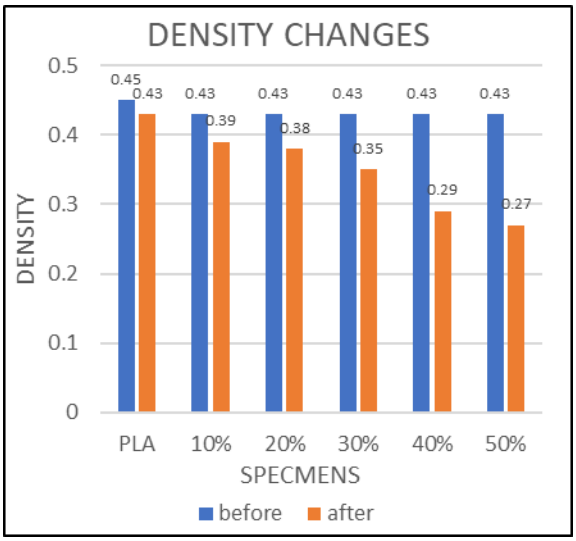


Figure 7: The density graph before and after the water submerged process.

Figure 7 shows the graph of the density before and after phase separation process for all the samples. The density value is essential for the porosity to be calculated theoretically using the equation (2). The density of the samples is affected by the etched PVA during the phase separation process. The graph before phase separation shows an almost constant value of 0.43 g/cm$^3$ irrespective of PVA content. The density value after the phase separation process, gradually decreased with the increment percentage of PVA ratio. The maximum decrease in density value was obtained with 50% of PLA/PVA samples. Unfortunately, the lowest density of a sample due to the highest porosity may reduce its mechanical properties.

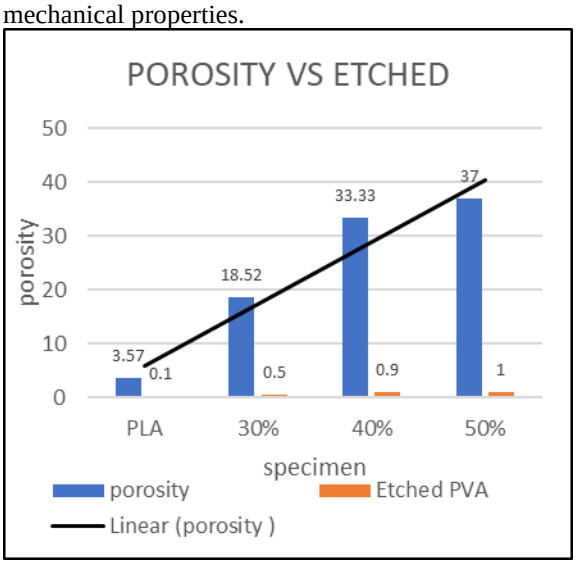


Figure 8: The porosity after the water submerged process.

.

Adversely, lower porosity is related to higher density in a sample. Figure 8 shows the graph of the porosity for all samples after the phase separation process. The result demonstrates that the PLA/PVA ratio of 30, 40 and 50% were 18.52, 33.33 and 37%, respectively. Those results show the correlation between the porosity and density.

In summary, Table 3 shows the relationship between the porosity and mechanical properties. The sample with 100% PLA content recorded higher mechanical properties than the samples with the presence of PVA. With presence of PVA in the samples, it induced the production of porosity which could affect the physical and mechanical properties. Previous studies also had demonstrated that higher PLA content led to higher tensile strength [26] - [28].

Table 4: The relationship between the porosity and mechanical properties.

| Code | Porosity, % | Density g/cm$^3$ | Stress, N/mm$^2$ | Force, N |
|---|---|---|---|---|
| PLA | 3.6 | 0.43 | 7.9 | 75.4 |
| S1 | 18.2 | 0.35 | 5.1 | 52.1 |
| S2 | 33.3 | 0.29 | 5.0 | 51.3 |
| S3 | 37 | 0.27 | 3.1 | 31.7 |

## CONCLUSION

This paper analyses feasibility of PLA/PVA composition in producing porosity for medical splinting devices by 3D printing process. A 3D printer occupied with a mixing nozzle of 2 filament inlets and 1 filament outlet hot end was used to print the compositions. The morphology, physical and mechanical properties were characterized and PLA/PVA ratio of 70/30 showed the best option for 3D splinting devices. The printed splinting devices will have acceptable breathable condition due to controlled porosity achieved by this study. This proved that a 3D printer occupied with a mixing nozzle is feasible and capable of producing PLA/PVA filament compositions with a desirable mixing ratio.

## ACKNOWLEDGMENTS

The authors wish to express their gratitude to the Ministry of Higher Education for funding this research (RACER/1/2019/TK03/UNIMAP//2). We would like to express our gratitude to all members of the Advance Material Processing & Design team who contributed directly or indirectly to this project.

**REFERENCES**


[1] Y. He, G. H. Xue, and J. Z. Fu, "Fabrication of low cost soft tissue prostheses with the desktop 3D printer," *Sci. Rep.*, vol. 4, pp. 1–7, 2014, doi: 10.1038/srep06973.

[2] D. Y. Nakamura, J. Niszezak, and J. A. Molnar, "Use of Silon-LTS® Low Temperature Splinting Material for Fabrication of a Scar Management Facial Orthosis in an Infant," *South. Reg. Burn Conf.*, vol. 8, no. 7, 2011.

[3] A. F. Aiman, M. N. Salleh, and K. A. Ismail, "Pressure distribution from two different types of fabrics head garments with Silon-LTS® face mask for hypertrophic burn scar treatment," *Proc. - 2015 2nd Int. Conf. Biomed. Eng. ICoBE 2015*, no. March, pp. 30–31, 2015, doi: 10.1109/ICoBE.2015.7235895.

[4] T. L. B. Pape, J. Kim, and B. Weiner, "The shaping of individual meanings assigned to assistive technology: a review of personal factors," *https://doi.org/10.1080/09638280110066235*, vol. 24, no. 1–3, pp. 5–20, Jan. 2009, doi: 10.1080/09638280110066235.

[5] M. M. Veehof, E. Taal, M. J. Willems, and M. A. F. J. Van De Laar, "Determinants of the use of wrist working splints in rheumatoid arthritis," *Arthritis Care Res. (Hoboken).*, vol. 59, no. 4, pp. 531–536, Apr. 2008, doi: 10.1002/ART.23531.

[6] H. Kim, G. H. Yang, C. H. Choi, Y. S. Cho, and G. H. Kim, "Gelatin/PVA scaffolds fabricated using a 3D-printing process employed with a low-temperature plate for hard tissue regeneration: Fabrication and characterizations," *Int. J. Biol. Macromol.*, vol. 120, pp. 119–127, Dec. 2018, doi: 10.1016/J.IJBIOMAC.2018.07.159.

[7] M. J. Pilley, C. Hitchens, G. Rose, S. Alexander, and D. I. Wimpenny, "The use of non-contact structured light scanning in burns pressure splint construction," *Burns*, vol. 37, no. 7, pp. 1168–1173, Nov. 2011, doi: 10.1016/J.BURNS.2011.07.005.

[8] M. A. Ahmad Fozi, M. N. Salleh, and K. A. Ismail, "Development of 3D-printed customized facial padding for burn patients," *Rapid Prototyp. J.*, vol. 25, no. 1, pp. 55–61, 2019, doi: 10.1108/RPJ-09-2017-0179.

[9] A. M. J. Paterson, "Digitisation of the splinting process-exploration and evaluation of a computer aided design approach to support additive manufacture," 2013. [Online]. Available: https://repository.lboro.ac.uk/articles/thesis/Digitisation_of_the_splinting_process_exploration_and_evaluation_of_a_computer_aided_design_approach_to_support_additive_manufacture/9350207. [Accessed: 05-Jun-2022].

[10] P. Saini, M. Arora, and M. N. V. R. Kumar, "Poly(lactic acid) blends in biomedical applications," *Adv. Drug Deliv. Rev.*, vol. 107, pp. 47–59, 2016, doi: 10.1016/j.addr.2016.06.014.

[11] K. Hamad, M. Kaseem, M. Ayyoob, J. Joo, and F. Deri, "Polylactic acid blends: The future of green, light and tough," *Prog. Polym. Sci.*, vol. 85, pp. 83–127, 2018, doi: 10.1016/j.progpolymsci.2018.07.001.

[12] K. H. Lee, D. K. Kim, Y. H. Cha, J. Y. Kwon, D. H. Kim, and S. J. Kim, "Personalized assistive device manufactured by 3D modelling and printing techniques," *Disabil. Rehabil. Assist. Technol.*, vol. 14, no. 5, pp. 526–531, 2019, doi: 10.1080/17483107.2018.1494217.

[13] J. Li and H. Tanaka, "Rapid customization system for 3D-printed splint using programmable modeling technique – a practical approach," *3D Print. Med.*, vol. 4, no. 1, Dec. 2018, doi: 10.1186/S41205-018-0027-6.

[14] F. Blaya, P. S. Pedro, J. L. Silva, R. D'Amato, E. S. Heras, and J. A. Juanes, "Design of an Orthopedic Product by Using Additive Manufacturing Technology: The Arm Splint," *J. Med. Syst.*, vol. 42, no. 3, 2018, doi: 10.1007/s10916-018-0909-6.

[15] G. Baronio, S. Harran, and A. Signoroni, "A Critical Analysis of a Hand Orthosis Reverse Engineering and 3D Printing Process," *Appl. Bionics Biomech.*, vol. 2016, 2016, doi: 10.1155/2016/8347478.

[16] H. S. Nam, C. H. Seo, S. Y. Joo, D. H. Kim, and D. S. Park, "The Application of Three-Dimensional Printed Finger Splints for Post Hand Burn Patients: A Case Series Investigation," *Ann. Rehabil. Med.*, vol. 42, no. 4, p. 634, Aug. 2018, doi: 10.5535/ARM.2018.42.4.634.

[17] C. H. Chu, I. J. Wang, J. R. Sun, and C. H. Liu, "Customized designs of short thumb orthoses using 3D hand parametric models," *https://doi.org/10.1080/10400435.2019.1709917*, vol. 34, no. 1, pp. 104–111, 2020, doi: 10.1080/10400435.2019.1709917.

[18] B. Kumar, J. Singh, A. Das, and R. Alagirusamy, "Comfort and compressional characteristics of padding bandages,"

*Materials Science and Engineering C*, vol. 57. pp. 215–221, 2015, doi: 10.1016/j.msec.2015.07.055.

[19] M. Behnezhad, M. Goodarzi, and H. Baniasadi, "Fabrication and characterization of polyvinyl alcohol/carboxymethyl cellulose/titanium dioxide degradable composite films: An RSM study," *Mater. Res. Express*, vol. 6, no. 12, 2019, doi: 10.1088/2053-1591/ab69cb.

[20] "Square & rectangle wargaming miniatures base collection by Mokanaman - Thingiverse." [Online]. Available: https://www.thingiverse.com/thing:1081926. [Accessed: 20-Oct-2022].

[21] ASTM D570, "Standard Test Method for Water Absorption of Plastics," *ASTM Stand.*, vol. 98, no. Reapproved 2010, pp. 25–28, 2014.

[22] N. Chuaponpat, T. Ueda, A. Ishigami, T. Kurose, and H. Ito, "Morphology , Thermal and Mechanical Properties of Co-Continuous Porous Structure of PLA / PVA Blends by Phase Separation," 2020.

[23] P. Pötschke and D. R. Paul, "Formation of co-continuous structures in melt-mixed immiscible polymer blends," *J. Macromol. Sci. - Polym. Rev.*, vol. 43, no. 1, pp. 87–141, 2003, doi: 10.1081/MC-120018022.

[24] "Standard Test Method for Tensile Properties of Plastics 1," doi: 10.1520/D0638-14.

[25] "Revised_ASTM_Tensile_Test_Specimen." [Online]. Available: https://www.thingiverse.com/thing:28987. [Accessed: 20-Oct-2022].

[26] B. M. Tymrak, M. Kreiger, and J. M. Pearce, "Mechanical properties of components fabricated with open-source 3-D printers under realistic environmental conditions," *Mater. Des.*, vol. 58, pp. 242–246, 2014, doi: 10.1016/j.matdes.2014.02.038.

[27] T. J. Gordelier, P. R. Thies, L. Turner, and L. Johanning, "Optimising the FDM additive manufacturing process to achieve maximum tensile strength: a state-of-the-art review," *Rapid Prototyp. J.*, vol. 25, no. 6, pp. 953–971, 2019, doi: 10.1108/RPJ-07-2018-0183.

[28] Manojit Das, Rajat Mishra, Palash Das, Sunil Kumar Kashyap, Sushanta Kumar Panda, "Controlled directionality in 3D printing of graphite-reinforced polymer composite with enhanced mechanical properties", *Composites Science and Technology*, Volume 235,109955,2023